Journal of Neurocytology **21**, 853–869 (1992)

Immunolocalization of B-50 (GAP-43) in the mouse olfactory bulb: predominant presence in preterminal axons

G. J. A. RAMAKERS[1]*, J. VERHAAGEN[1]**, A. B. OESTREICHER[1], F. L. MARGOLIS[2], P. M. P. VAN BERGEN EN HENEGOUWEN[3] and W. H. GISPEN[1]

[1] *Rudolf Magnus Institute, University of Utrecht, Vondellaan 6, 3521 GD Utrecht, The Netherlands*
[2] *Laboratory of Chemosensory Neurobiology, Roche Institute of Molecular Biology, 340 Kingsland Street, Nutley, NJ 07110–1199, USA*
[3] *Department of Electron Microscopy, University of Utrecht, Padualaan 8, 3554 CH Utrecht, The Netherlands*

Received 6 January 1992; revised 22 June and 28 July 1992; accepted 28 August 1992

Summary

Because the growth-associated protein B-50 (GAP-43) has been implicated in neurite outgrowth as well as in synaptic plasticity, we studied its light and electron microscopical distribution in the mouse olfactory bulb, an area of the nervous system which exhibits a high degree of synaptic plasticity. Immunofluorescent staining with monospecific affinity-purified anti-B-50 antibodies revealed that B-50 is most abundantly expressed in the olfactory nerve fibre layer and the granule cell layer neuropil, while little staining was observed in the external plexiform layer and in cell bodies. B-50 is absent from dendrites and myelinated axons as indicated by double labelling with monoclonal antibodies against microtubule-associated protein 2 and the large neurofilament protein, respectively. Using post-embedding immunogold labelling on ultrathin Lowicryl sections, B-50 was found to be highly concentrated in presumed growth cones in the olfactory nerve fibre layer and in thin unmyelinated axons and presynaptic terminals in the granule cell layer neuropil. Near background immunolabelling was seen in perikarya, dendrites and myelinated axons. In view of the implication of B-50 in plasticity-related phenomena, its abundance in the thin unmyelinated preterminal axons suggests that these are potential sites of extrasynaptic plasticity.

Introduction

The neural-specific phosphoprotein B-50, also known as GAP-43, neuromodulin, F1, or pp46 (Benowitz & Routtenberg, 1987), has been associated with neurite outgrowth (Skene & Willard 1981a,b), neurotransmitter release (Dekker *et al.*, 1989b), and synaptic plasticity (Lovinger *et al.*, 1985). B-50 is a prominent substrate of protein kinase C (Kratz *et al.*, 1985, Van Hooff *et al.*, 1988, Dekker *et al.*, 1989a), and it modulates several second messenger systems (Skene, 1989). B-50 affects the formation of phosphatidylinositol bisphosphate (Gispen *et al.*, 1985), from which the second messenger inositol trisphosphate (IP_3) is generated, and is able to bind to calmodulin (Alexander *et al.*, 1987). In addition B-50 enhances the binding of GTP to a G_0-protein (Strittmatter *et al.*, 1990).

In early postnatal brain (De Graan *et al.*, 1985; Skene *et al.*, 1986) and in neuronal tissue culture (Meiri *et al.*, 1986, 1988; Ramakers *et al.*, 1991b) B-50 is most prominently expressed in neuronal growth cones and in distal axons, where it might operate to translate extracellular signals to the growth cone cytoskeleton to mediate directed outgrowth (Ramakers *et al.*, 1991c). In adult brain, B-50 levels are relatively high in areas thought to exhibit a high degree of synaptic plasticity, including the hippocampus and association areas in the cortex (Neve *et al.*, 1988; Benowitz *et al.*, 1988; De la Monte *et al.*, 1989). B-50 is present in presynaptic terminals (Gispen *et al.*, 1985; DiFiglia *et al.*, 1990) and in unmyelinated fibres and in dendritic spines in the neostriatum (DiFiglia *et al.*, 1990). Studies with antibodies that can discriminate between phosphorylated and dephosporylated B-50 have shown that the protein becomes phosphorylated during axonal transport (Meiri *et al.*, 1991).

An area of the adult mammalian nervous system where extensive synaptic plasticity occurs is the olfactory system. The anatomical relationships between

* Present address: Molecular Biology and Virology Lab, Salk Institute, P.O. Box 85800, San Diego, CA 92138–9216, USA.
** To whom correspondence should be addressed

0300–4864/92 $03.00 +.12

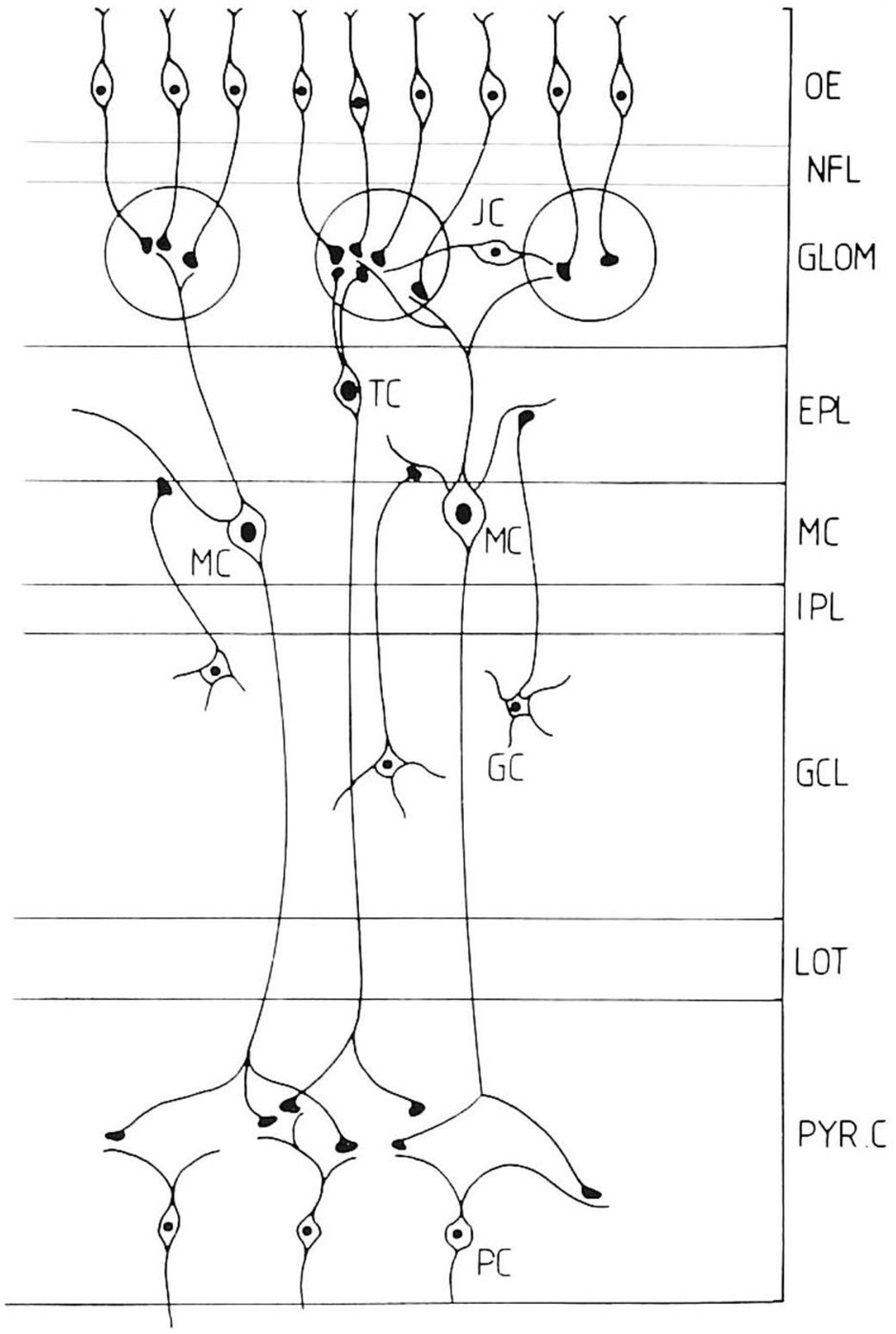

Fig. 1. Illustration of the anatomical relations between the neurons in the olfactory system. The primary olfactory neurons are located in the olfactory epithelium (OE). Their axons penetrate the cribriform plate forming the nerve fibre layer (NFL) and project into the olfactory bulb glomeruli (GLOM) where they form synapses on the dendrites of the tufted cells (TC) and mitral cells (MC). The glomeruli are surrounded by juxtaglomerular neurons (JC). The external plexiform layer (EPL) is mainly composed of mitral and tufted cell dendrites. The mitral and tufted cells project their axons through the internal plexiform layer (IPL) and in between the granule cell (GC) in the granule cell layer (GCL) thus forming the lateral olfactory tract (LOT). Mitral cell axons form synapses on the pyriform cells (PC) in the pyramidal cortex (PYR C).

various olfactory bulb neurons is illustrated in Fig. 1. Primary olfactory neurons in the olfactory neuroepithelium are continuously generated from stem cells to replace degenerating neurons in the outer layers of the epithelium. Thus, there is continuous turn-over of their synaptic connections on dendrites of mitral cells, tufted cells and periglomerular cells (Graziadei & Monti-Graziadei, 1978). The developmental and synaptic plasticity of olfactory neurons is reflected in the continued expression of developmental markers, including vimentin (Schwob *et al.*, 1986), the embryonic neural cell adhesion molecule (Miragall *et al.*, 1988), and microtubule-associated proteins MAP2c, MAP5a and 'juvenile' tau (Viereck *et al.*, 1989). B-50 is specifically expressed in newly formed primary olfactory neurons in the adult olfactory epithelium (Verhaagen *et al.*, 1989, 1990a). In the main olfactory bulb (MOB), this was reflected in punctate B-50-immunostaining of the incoming primary olfactory axons, which form the nerve fibre layer of the MOB. Mitral and periglomerular cells in the olfactory bulb expressed high levels of B-50 mRNA in young adult (Rosenthal *et al.*, 1987; De la Monte *et al.*, 1989) and aging animals (Verhaagen *et al.*, 1990a). We proposed that this high expression of B-50 mRNA could reflect plastic responses of the mitral cells to the turn-over of connections between primary olfactory axon terminals and mitral cell dendrites in the glomeruli of the MOB. On the other hand, the persistent expression of B-50 mRNA in mitral cells may be related to synaptic plasticity of mitral cell synapses in the piriform cortex (Verhaagen *et al.*, 1990a).

To investigate further these possibilities, we carried out a detailed study on the localization of B-50 in the mouse MOB, by comparing its light microscopic distribution with that of specific marker proteins: olfactory marker protein (OMP), a protein expressed in mature primary olfactory neurons (Farbman & Margolis, 1980), MAP2, a dendritic marker absent from axons (Bernhardt & Matus, 1984), and the high molecular weight neurofilament protein (Ramakers *et al.*, 1991a), specific for myelinated axons. Furthermore, the ultrastructural distribution of B-50 was investigated, using postembedding immunostaining with gold probes on Lowicryl-embedded MOB. B-50 expression is most prominent in a subset of olfactory axons and in their presumptive growth cones in the nerve fibre layer, in unmyelinated axons in the granule cell layer and in the projection areas of mitral cells in the pyriform cortex.

Materials and methods

Fixation and tissue preparation

Six-week-old mice of the FVB strain were injected with 100 IU of heparin and anaesthetized with 50 µl Narcovet. Subsequently, they were perfusion fixed for 15 min at a rate of 8 ml min^{-1} with 4% paraformaldehyde in PBS (10 mM phosphate buffer (pH 7.3) in 0.9% saline, 37° C) for immunofluoresence ($n = 2$) or with 100 ml of 2% glutaraldehyde (Polysciences Inc., biological grade, Warrington, USA) and 4% paraformaldehyde (BDH, Poole, UK) in PBS for EM ($n = 2$). After removal, fixation of the brains with attached olfactory bulbs was continued overnight at 4° C. For immunofluorescence, the brains were infused with 10, 20 and 30% sucrose in PBS at 4° C until they sank, and subsequently frozen in 10 ml of isopentane in a small container on liquid

nitrogen. After storage at −80° C, 5 μm sections were cut in a Bright cryostat (Huntingdon, England), mounted on gelatin/potassium chromo sulfate ($KCr(SO_4)_2$).12 H_2O (1%1% w/v) coated slides and immunostained.

For EM, 100 μm coronal sections of the olfactory bulb and cortex were cut on a vibratome (Micro Cut H1200, Bio-Rad) and subsequently processed for conventional EM, or for immuno-EM. For conventional EM, the sections were post-fixed in 2% OsO_4 for 2 h and embedded in Epon. For immuno-EM, the procedure of Van Lookeren Campagne and colleagues (1991a) was slightly modified. Briefly, the sections were subsequently incubated in 10, 20 and 30% glycerol in PBS for 30 min each, after which small pieces of 1 × 2 mm were dissected from them. These were mounted between a plastic thermanox disk with a diameter of 3.5 mm (LAB-TEK, Miles Laboratories, Naperville, USA) and a copper holder, separated from each other by a 100 μm spacer, ultra-rapidly frozen in liquid nitrogen slush (−210° C), and stored in liquid nitrogen. The frozen tissue preparations were embedded in Lowicryl HM20 (Chemische Werke Lowi, Balzers, Waldkraiburg, FRG), in a 'CS auto' freeze substitution apparatus (Reichert-Jung, FRG) using the freeze-substitution procedure of Humbel and Müller (1986). Briefly, the tissue preparations were infused with 0.5% uranyl acetate in methanol (w/v) for 36 h at −90° C and then brought to −45° C at a rate of 4° C per h. The methanol was exchanged for pure Lowicryl HM20 in four steps: 2 h in 50% methanol/50% HM20 (v/v); 2 h in 33% methanol/67% HM20; overnight in pure HM20; followed by another 2 h in fresh HM20. The HM20 plastic was polymerized at −45° C under UV-light for 48 h. Following a final hardening under UV light for 24 h at room temperature, the embedded tissue was trimmed, and ultrathin sections (70 nm) were prepared using and LKB diamond knife. The ultrathin sections were collected on 3.5 mm non-coated nickel EM grids, to obtain maximum contrast in the EM.

Immunofluorescence staining procedures

Before staining, remaining aldehyde groups were quenched with 50 mM glycine in PBS with 0.05% Triton X-100 (PBS-T) for 30 min. Subsequently, all steps were performed in PBS-T containing 0.5% gelatin (PBS-TG). Following two 10 min washes, the sections were incubated overnight with the primary antibodies in 100 μl PBS-TG at 4° C, washed 6 × 15 min, incubated for 1 h with the secondary antibodies in 100 μl PBS-TG, and washed 4 × 15 min. Finally, the sections were washed 3 × 10 min with PBS, stained for 1 min with the Hoechst stain (for fluorescent nuclear counterstaining), washed again 3 × 5 min with PBS, and mounted in DABCO mounting medium consisting of 25% glycerol, 10% (w/v) Mowiol 4–88 (Hoechst, Frankfurt, FRG) and 0.1% (w/v) 1,4 diazabicyclo-(2,2,2)-octane (DABCO; Janssen, Beerse, Belgium) in 0.1 M Tris/HCl (pH 8.5). For B-50 staining, affinity-purified rabbit IgG No. 8613 was used at a dilution of 1:200 (0.1 ng ml^{-1}; Oestreicher *et al.*, 1983). Goat-anti-rat OMP antiserum was used 1/4000 (Margolis, 1972; Monti-Graziadei *et al.*, 1977). The mouse monoclonal antibody AP14 recognizing MAP2 was used 1/50. The mouse monoclonal RNF402, raised against a neurofilament preparation of human spinal cord, and specific for the 200 kDa neurofilament (H) subunit was used at a 1:10 dilution (Ramakers *et al.*, 1991a). Secondary antibodies used were: donkey-anti-rabbit coupled to fluoroisothiocyanate (FITC), and donkey-anti-goat, and goat-anti-mouse, both coupled to Texas Red sulfonyl chloride. All were affinity-purified and used at a dilution of 1:100 (Jackson Immunoresearch, West Grove, PA, USA). For immunofluorescent double staining, both primary and secondary antibodies were incubated simultaneously at the same concentrations as when used separately. Cross-staining of any of the primary antibodies with the other secondary antibodies was completely negative. Staining patterns in the double staining procedure were exactly the same as in single staining. Deletion of the primary antibody in all cases resulted in a negligible background staining. Immunostaining with pre-immune IgG No. 8613, or after overnight pre-absorption of B-50 IgG No. 8613, diluted 1:200, with an excess (1 μg ml^{-1}) purified B-50 protein at 4° C, resulted in negligible background staining (not shown).

Stained sections were examined using a Leitz Orthoplan microscope with Ploemopak 2 epifluorescence optics and filter combinations for FITC, rhodamine and Hoechst fluorescence. Photographs were made with a Wild MPS 45 Photoautomat using Kodak TriX pan 400 film exposed at 1600 ASA.

Postembedding immunogold labelling procedures

For postembedding immunogold staining, the procedure described by Van Bergen en Henegouwen (1989) was slightly modified. The nickel grids were incubated, with the ultrathin sections face-down, on 25 μl drops of PBS containing 50 mM glycine and 0.1% (w/v) borohydride for 30 min to quench any remaining aldehyde groups, and washed on five drops of PBS for 5 min each. Subsequently, the sections were incubated on drops of PBG (PBS containing 0.5% bovine serum albumin fraction V and 0.2% gelatin): 4 × 45 min on PBG alone, overnight with 10 μl of the diluted primary antibody at 4° C, 10 × 45 min on PBG, overnight again on 10 μl of diluted goat-anti-rabbit IgG coupled to 1 or 10 nm gold particles (Janssen Pharmaceutica, Beerse, Belgium) at 4° C, and thereafter 10 × 5 min on PBG. Following 5 × 5 min incubations on PBS, the sections were postfixed on drops of 2% glutaraldehyde for 15 min, and rinsed on five drops of milliQ purified water. If no silver enhancement step was required, the sections were air dried and later stained with saturated uranyl acetate and lead citrate, for 10 and 1 min, respectively. When required, silver enhancement was done according to Danscher (1981) for 12 min in the dark at 26° C, followed by contrasting with uranyl acetate and lead citrate as above. With this procedure, 1 nm gold particles were enlarged to about 10 nm. The conventional and immuno-stained sections were examined in a Philips EM300 microscope and photographed at a magnification of × 16 000.

B-50 IgG No. 8613 was used at a dilution of 1/50 to 1/200 in combination with 10 nm and 1 nm immunogold particles, respectively. The OMP antiserum was used at 1/8000 in combination with 10 nm gold particles, which were further silver-enhanced. As the OMP antiserum was produced in a goat, a 'bridging step' was added: after overnight incubation with the OMP antiserum, the grids were washed 10 × 5 min on PBG, incubated in rabbit-anti-goat antibodies (1/500; Nordic) for 6 h at 4° C, washed 10 × 5 min on PBG, and further incubated with goat-anti-rabbit IgG coupled to 10 nm gold particles as above. In both procedures, deletion of the

primary antibody resulted in a negligible background labelling. A similar low background was seen with pre-IgG No. 8613 (1/50) or with IgG No. 8613 diluted 1/50, and preabsorbed overnight at 4° C with 1 μg ml^{-1} purified B-50 protein (not shown).

As a further control of the specificity of the B-50 affinity-purified IgG No. 8613, 10 μg of total protein of 6-week-old mouse MOB was separated on 11% SDS-polyacrylamide gels, (Western) blotted onto nitrocellulose, and immunostained with a concentration range of IgG No. 8613 of 1/200 to 1/1600, using diaminobenzidine as chromogen (Van der Sluis *et al.*, 1987). Immunostaining was also performed after 2 h postfixation of the blots with 2% glutaraldehyde and 4% paraformaldehyde, to check for possible introduction of cross-reactivity by the fixatives used. In both cases, only a single band was stained which corresponded in molecular weight to that of purified B-50. This band was completely abolished when the IgG No. 8613 was preabsorbed as above. Thus, the IgG No. 8613 fulfills the most stringent conditions for monospecific B-50 staining in the MOB under the fixation conditions used.

Quantification of immunogold labelling densities

Several considerations with regard to counting and calculating B-50 labelling densities in the various structures of the MOB have been taken into account. First, for quantitative purposes, labelling with 10 nm particles was more suitable than labelling with 1 nm particles. Although both specific and background labelling density with the small particles was higher, 1 nm immunogold particles were found to form aggregates of up to 10 particles, resulting in a much lower spatial resolution than with 10 nm particles. As this proved to be especially problematic with membrane-associated labelling (see below), we only used 10 nm particles for quantitative purposes, which have an estimated spatial resolution of 20 nm (Ottersen, 1989). Second, as previous EM work has shown, B-50 is to a large part, but not completely, membrane-associated (Van Lookeren Campagne *et al.*, 1991a). Thus, B-50 labelling was expressed relative to both membrane length and structure surface area. Third, since most membranes are very closely apposed to the membranes of neighbouring structures, and the resolution of 10 nm immunogold particles is about twice the thickness of the plasma membrane, membrane-associated labelling could be derived from both apposed membranes. For instance, although in the granule cell layer two apposed granule cell plasma membranes show very low labelling, a granule cell plasma membrane may appear to be rich in labelling, when apposed by highly labelled thin unmyelinated axons. The same applies to (postsynaptic) dendritic structures and thin unmyelinated axons in this layer, as can be seen most clearly when 1 nm gold particles are used (see Fig. 7). Thus, membrane-associated B-50 labelling was expressed relative to both apposed plasma membranes and divided by two. In cases where structures of the same type were apposed, this yielded the 'true' membrane density of that structure (for instance using apposed plasma membranes of granule cells, or apposed membranes of thin, unmyelinated axons in the granule cell layer or fibre layer). In cases where structures are always bordered by structures of another type (e.g. myelinated axons), the 'mixed' value has been given.

'Total surface density' was calculated by expressing all gold particles within a (membrane-delineated) structure relative to its profile area. For this parameter, gold particles on the plasma membrane were assigned to the structure they were nearest to. 'Membrane-associated labelling' included all particles that were found within 20 nm on either side of the apposed membranes, relative to the total membrane length. 'Cytoplasmic labelling density' included all non-membrane-associated gold particles (more than 20 nm away from the plasma membrane) relative to the 'surface area'.

Photographs were taken at random throughout the MOB and printed at a final magnification of × 80 000. The only selection criterion that was applied to the photographs was, that the membranes should have enough contrast to be well visible. One exception was made for growth cone like structures. Since these were rather scarce, each growth cone encountered was photographed separately. Gold particles (10 nm) were counted by hand, and assigned to a certain structure or membrane. Membrane lengths and surface areas were measured using a Calcomp 2000 graphics tablet, linked to a HP9000/835 computer. The different parameters were computed for each continuous membrane length and structure area as indicated above. Since all parameters are ratios of numbers of gold particles and membrane lengths or surface areas, statistical comparisons were made by non-parametric statistics. For comparison of two groups, the Mann-Whitney U-test was used, for more than two groups, the Kruskall-Wallis test was used (Siegel & Castellan, 1988).

Results

Light microscopic localization of B-50 in relation to olfactory marker protein and dendritic and axonal markers

To delineate the cellular and subcellular location of B-50 in the mouse MOB, B-50 staining was compared (in the same section) to the location of several proteins specific for either mature primary olfactory neurons (OMP), dendrites (MAP2) or myelinated axons (NFH). Intense staining for OMP occurred exclusively in the fibre layer and in patches within the glomeruli, filling approximately 80 to 90% of the glomerular surface area (Fig. 2B). This staining pattern is consistent with an exclusive localization of OMP in the axons and terminals of primary olfactory neurons within the olfactory bulb (Monti-Graziadei *et al.*, 1977). Staining for MAP2 was most prominent in the external plexiform layer, where it was located in dendritic branches of varying thickness, some of which extended into the glomeruli and into the periglomerular area (Fig. 3B). A fairly high density of somewhat thinner MAP2-stained dendrites was seen throughout the granule cell layer, crossing the internal plexiform layer into the external plexiform layer. No MAP2 staining was observed in the fibre layer. Staining for the high molecular weight (200 kDa) neurofilament protein with two different monoclonal antibodies, revealed a

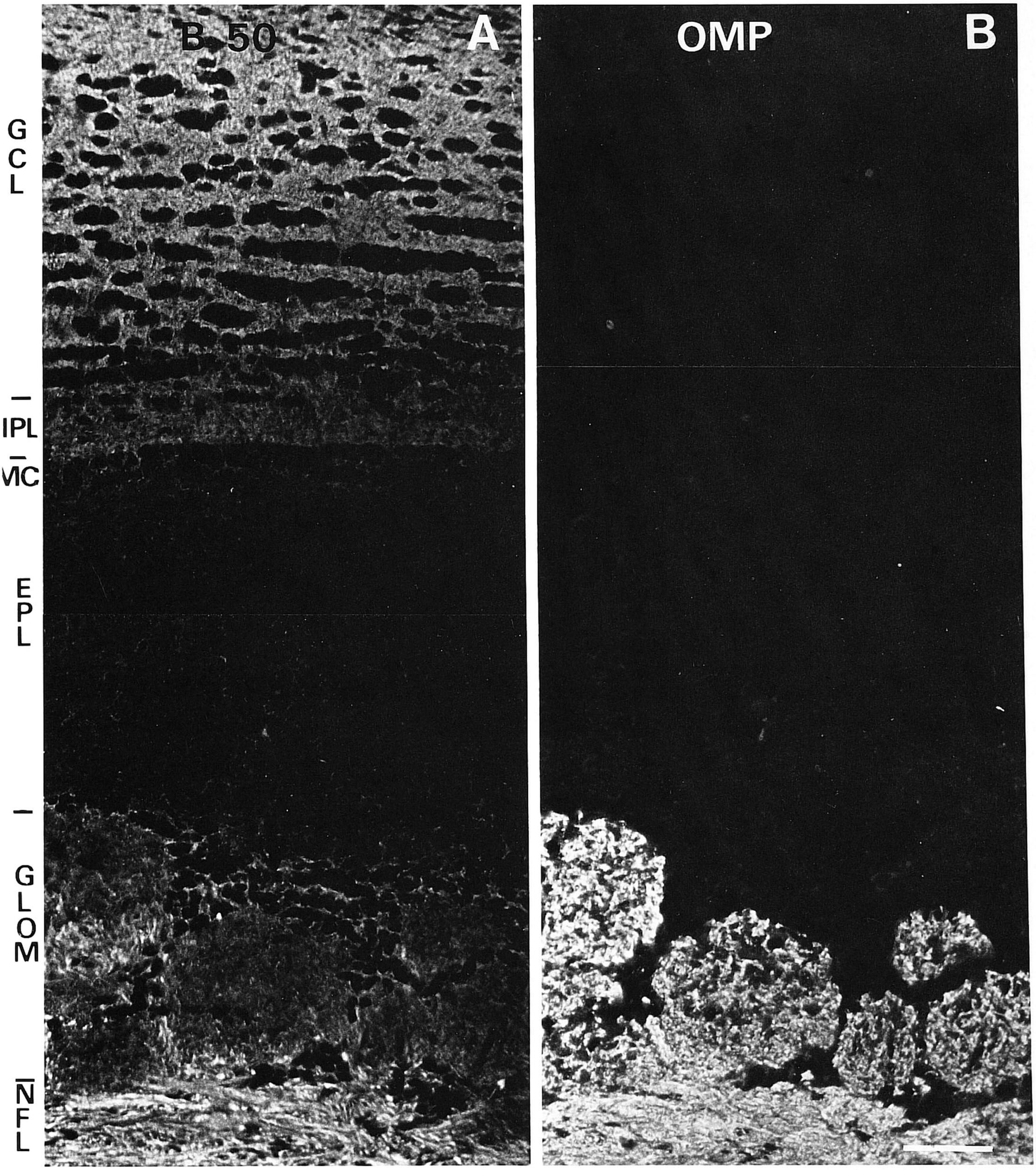

Fig. 2. Immunofluorescent double staining for B-50 (A) and OMP (B) in an olfactory bulb of a six-week-old mouse. Note that staining from OMP in the glomeruli has the same intensity as in the fibre layer, whereas the intensity of B-50 staining decreases when the primary olfactory axons go deeper into the glomeruli. Abbreviations as in Fig.1. Scale bar = 50 μm.

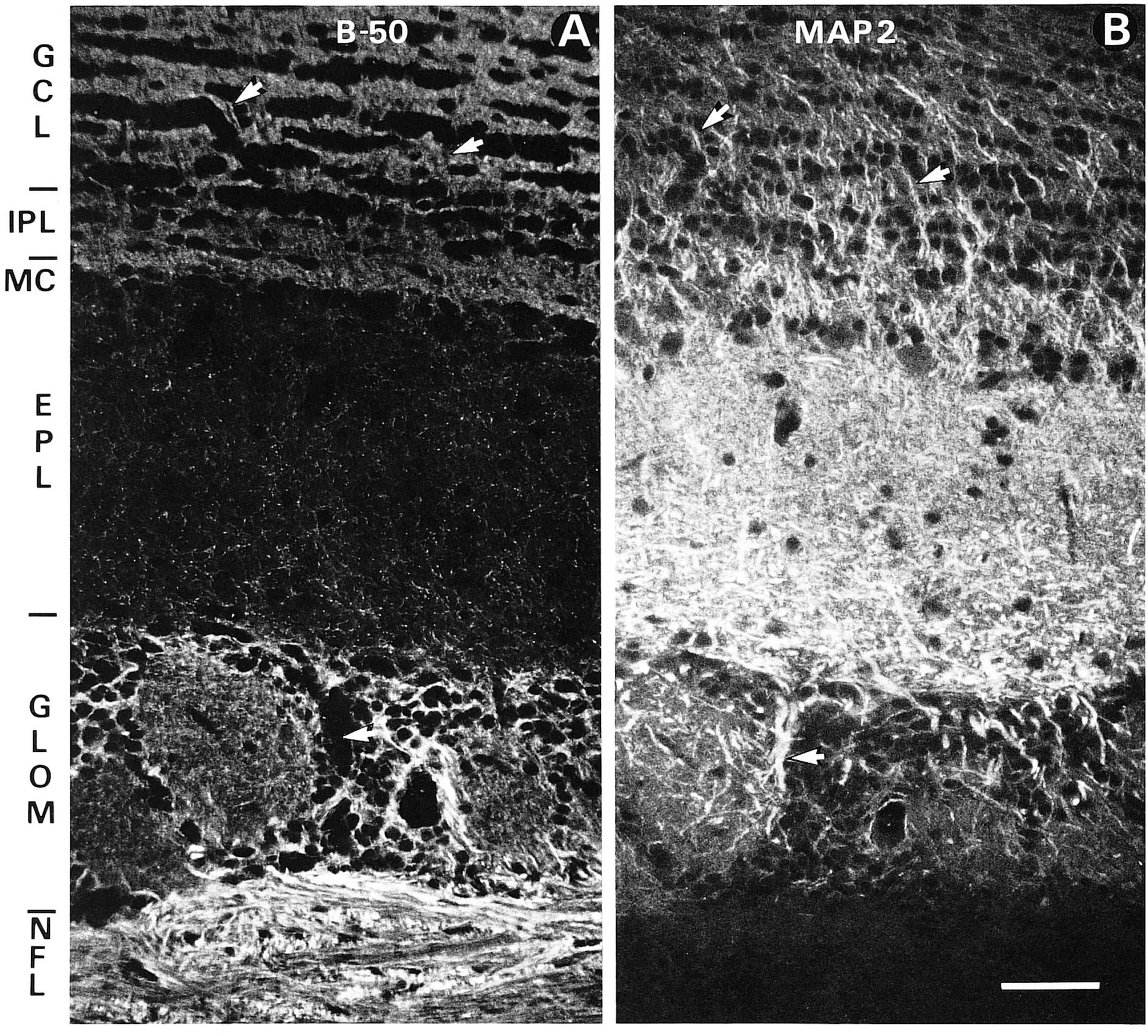

Fig. 3. Immunofluorescent double staining for B-50 (A) and MAP2 (B) of six-week-old olfactory bulb. Note the complementarity of staining of B-50 and MAP2 in all layers. The arrowheads indicate heavily MAP2-stained dendrites in the glomerular layer and granule cell/internal plexiform layer in (B) which are associated with low staining for B-50 in (A). Abbreviations as in Fig. 1. Scale bar = 50 μm.

high density of thin fibres or puncta in the internal plexiform layer, and a variable density of clusters of puncta in the granule cell layer, just above the internal plexiform layer (Fig. 4B). Throughout the rest of the granule cell layer, NFH positive puncta were scattered in between the islands of granule cell bodies. A very low density of NFH stained thin fibres or puncta also existed in the external plexiform layer and among the periglomerular cells, but no NFH staining was observed in the fibre layer. The distribution of NFH

Fig. 4. Combined immunofluorescent staining in the MOB for B-50 (A) and NFH (B) and for MBP (C) and NFH (D). Note the very low staining of B-50 in A (arrowheads) at cross-sectioned bundles of NFH-positive myelinated axons in B (arrowheads). In addition, the lower overall staining intensity for B-50 in the internal plexiform layer relative to the deeper part of the GCL (see also Figs. 1A and 2A) in (A), is complementary to the density of NFH-positive myelinated axons in the internal plexiform layer and GCL. Panels (C) and (D) illustrate the colocalization of NFH and MBP. Abbreviations as in Fig. 1. Scale bar = 50 μm.

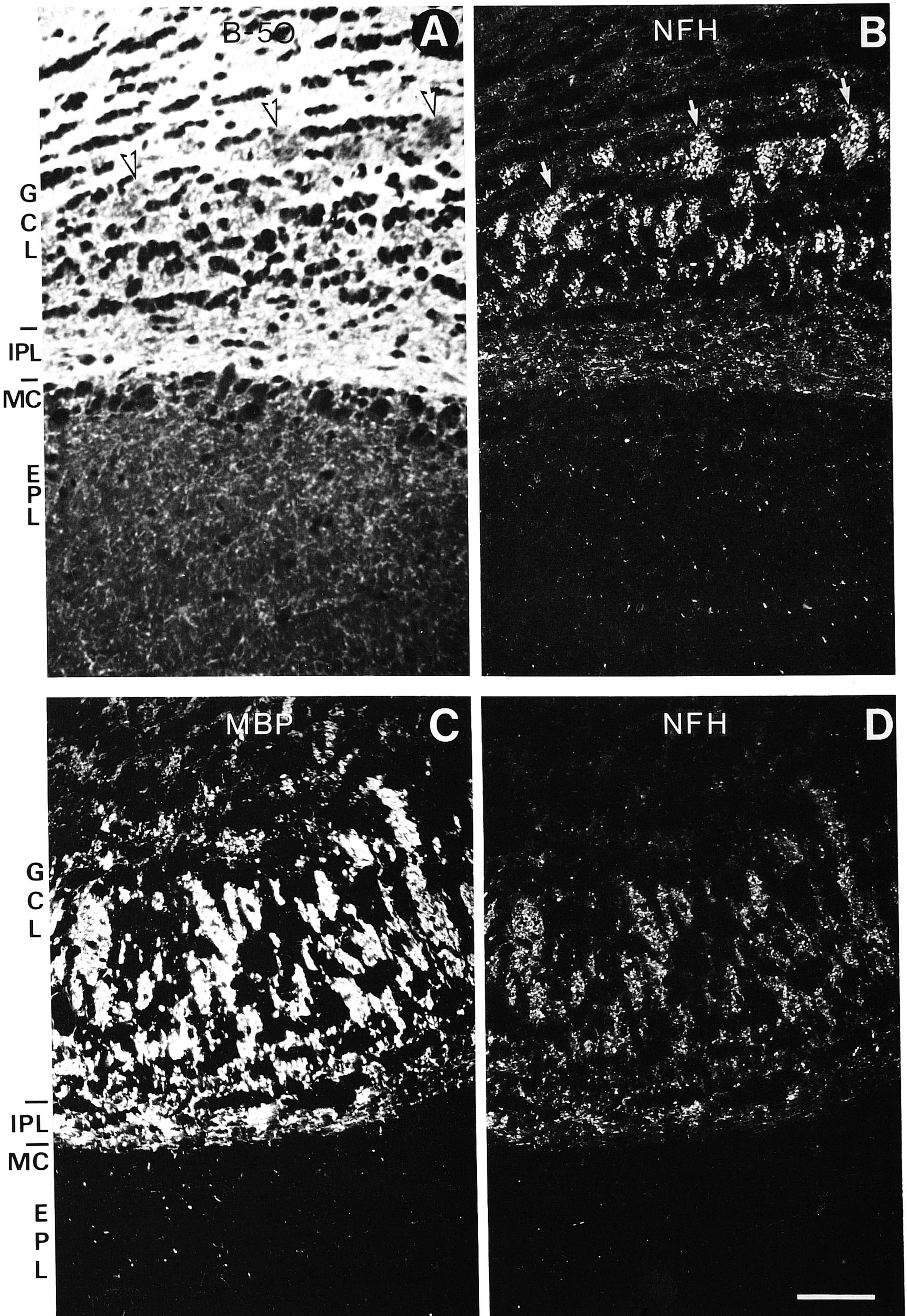
B-50
A
NFH
B
GCL
IPL
MC
EPL
MBP
C
NFH
D
GCL
IPL
MC
EPL

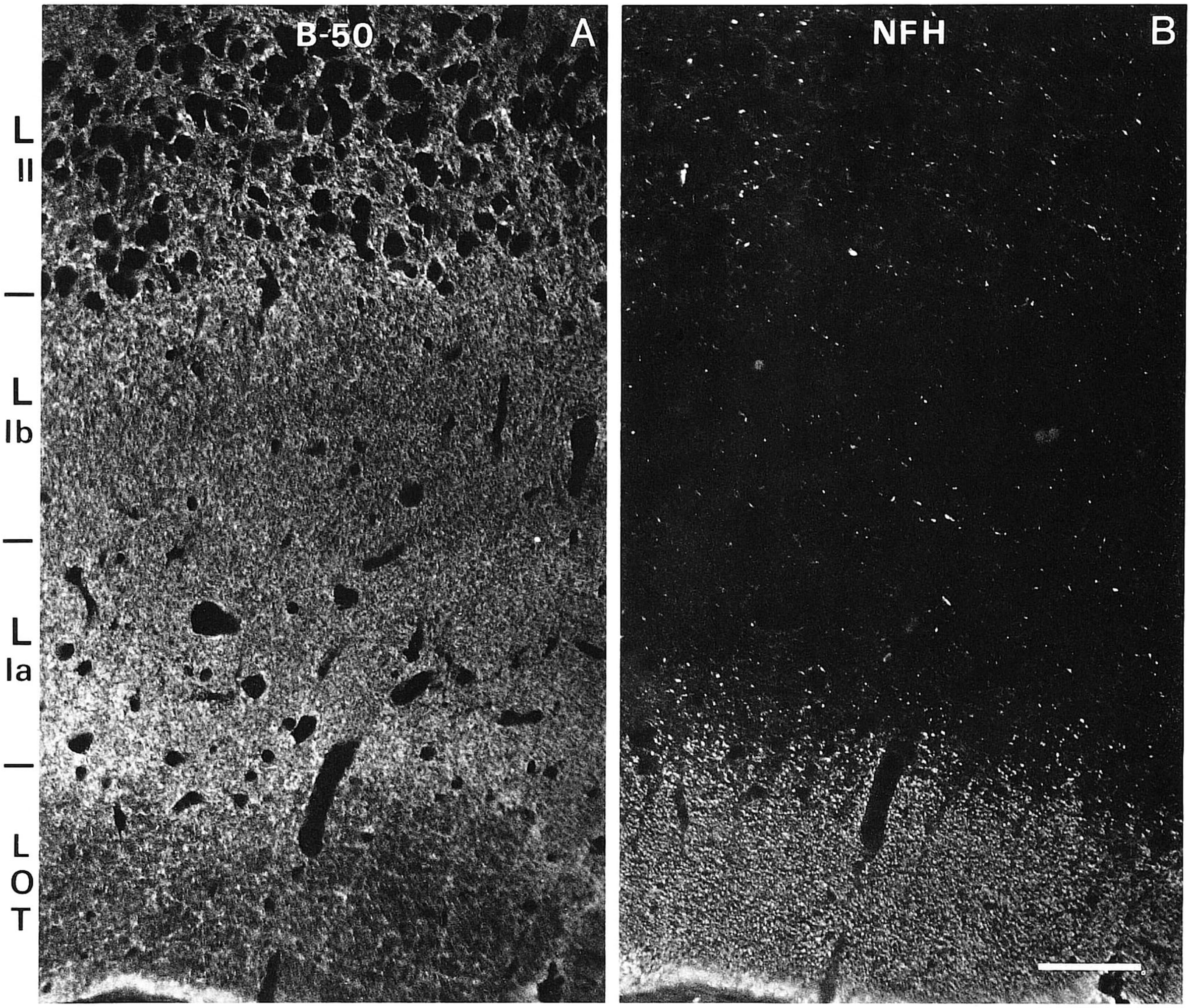

Fig. 5. Immunofluorescent double staining for B-50 (A) and NFH (B) in six-week-old piriform cortex. Note the low staining intensity for B-50 in the LOT (A), which shows a high density of cross-sectioned NFH-positive myelinated axons (B). The highest staining intensity for B-50 is observed in the border region between the LOT and layer Ia, and the upper part of layer Ib and the lower part of layer II, between the pyramidal neurons. LOT: lateral olfactory tract; L Ia, L Ib and L II: layers Ia, Ib, and II of the piriform cortex, respectively. Scale bar = 50 μm.

staining appeared to correspond to that of myelinated axons in the MOB (and other parts of the brain: not shown). This was verified by double staining of the MOB using neurofilament antibody and a rabbit antiserum against myelin basic protein (MBP). The distribution of small NFH puncta or thin NFH fibres was matched by somewhat larger MBP-positive puncta or fibre-like structures in all areas investigated , including the MOB (Fig. 4C, D). Switching from the rhodamine filter pair to the FITC filter pair, clearly showed the MBP staining surrounding the NFH staining, confirming the exclusive location of the NFH antigen recognized by our antibodies within myelinated axons.

Immunofluorescent staining for B-50 in the MOB showed the highest labelling intensities in the nerve fibre layer (containing the axons of the primary olfactory neurons), in the external parts of the glomeruli, and in the granule cell layer (Figs 2A, 3A, 4A). A somewhat less intense staining was observed among the periglomerular cells and in the internal plexiform layer. Intermediate to low staining was seen in the

main part of the glomeruli, whereas the external plexiform layer showed the lowest overall staining intensity.

Within the nerve fibre layer, B-50 staining exhibited a somewhat patchy staining pattern. Most, but not all olfactory axons (Fig. 2A; compare with OMP staining: Fig. 2B) were immunoreactive. The patchy staining of the olfactory fibre layer became more pronounced with time as seen in six-month-old mice (data not shown). The olfactory axons were always grouped together in bundles which were sectioned longitudinally or transversely. Overall staining intensity could vary considerably from one bundle to the next. Upon entering the glomeruli, the OMP-positive (Fig. 2B) olfactory axons remained strongly stained, but deeper into the glomeruli, the intensity of B-50 staining appeared drastically reduced (compare Fig. 2A and 2B). The cell bodies of the periglomerular cells surrounding the glomeruli (Fig. 2C) showed only background staining, but were surrounded by B-50 positive fibres (Fig. 2A). The external plexiform layer showed the lowest overall intensity of B-50 staining in the MOB, except for a low density of thin B-50 positive fibres (Figs 2–4A). The mitral cells located at the border between the external and internal plexiform layer also did not show any staining, but their circumference sometimes was outlined by B-50 stained fibres coursing around them. In the internal plexiform layer, relatively intense, punctate B-50 staining was observed in between unstained cell bodies and dendritic trunks originating from granule cells. In the neuropil of the granule cell layer, B-50 staining was as intense as in the fibre layer, outlining the islands of unstained granule cells (Figs 2A–5A). The deeper part of the granule cell layer was always stained somewhat more intensely than the superficial part.

When comparing the distribution of B-50 to that of the dendritic marker, MAP2, an almost complete complementarity was observed (compare Fig. 3A, B). Only in the granule cell layer and internal plexiform layer was this complementarity somewhat less clear-cut. However, upon careful inspection, a lower staining for B-50 could be seen at sites where the relatively thin MAP2-stained dendritic trunks of granule cells projected to the external plexiform layer. In the same layers, a complementarity was seen between B-50 staining and the staining with the NFH antibodies (Fig. 4A, B), with B-50 staining being of lower intensity at areas with a high density of NFH stained axons (i.e. the internal plexiform layer and loose bundles of axons within the superficial granule cell layer).

To characterize the projection of the axons of the mitral and tufted cells to the piriform cortex, one of the major central projections of these neurons, sections of piriform cortex were double stained for B-50 and the NFH protein. In the piriform cortex, intense staining for NFH was seen in the lateral olfactory tract (LOT), containing the myelinated mitral and tufted cell axons (Fig. 5B). Throughout layers I and II (and III: not shown) scattered fibre-like and punctate NFH staining was observed. In contrast to NFH staining, B-50 staining showed the lowest intensity in the LOT (Fig. 5A, B). The highest intensity of B-50 staining in the piriform cortex was consistently observed in the area bordering the LOT and layer Ia and in the region of layer Ib just below the pyramidal cell bodies in layer II.

Electron microscopic localization of B-50

When the MOB was postfixed with OsO_4 and embedded in Epon an optimal preservation of morphological detail was retained, with nicely contrasted membranes (not shown). However, postembedding staining for B-50 resulted only in very low density background staining (not shown). In contrast, when the same tissue was freeze-substituted and embedded in Lowicryl, a reasonable preservation of morphology was obtained, together with a good retention of B-50 antigenicity. However, morphological contrast was less than with osmium-fixed tissue embedded in Epon, as membranes were less electron-dense. As a result, synaptic vesicles were more difficult to discern. To check for non-specific and background staining, Lowicryl sections of MOB were immunostained in the absence of the first antibody, or in the presence of either pre-immune IgG, or in anti-B-50 IgG 8613, preabsorbed with 1 $\mu g\,ml^{-1}$ purified B-50. In all three cases, a very low staining density was observed throughout all layers of the MOB (not shown); this level of staining will further be denoted as 'background'.

Upon staining with anti-B-50 IgG, a moderately high density of gold labelling was observed in the nerve fibre layer (Fig. 6A, C–E), exhibiting some regional variability. Part of the staining was found in close proximity to the plasma membrane, but a fair amount appeared to be cytoplasmic (Fig. 6A, Table 1). Background labelling was observed in the ensheathing glial cells (Fig. 6A). Occasionally, scattered throughout the fibre layer, structures were observed which contained a high density of gold labelling (Fig. 6C–E). These were usually irregular in shape, and sometimes contained abundant membranous organelles. Some of these profiles showed a larger diameter than the olfactory axons, and contained B-50 labelling throughout or mainly along the plasma membrane (Fig. 6C). B-50-enriched structures with a similar thickness as the olfactory axons showed a very high labelling density throughout. Apart from one exception, such highly labelled structures were not observed outside the areas that contained olfactory axons.

In the glomeruli, olfactory axon terminals could be easily distinguished from dendritic structures by their relatively high electron density, resulting from a dense

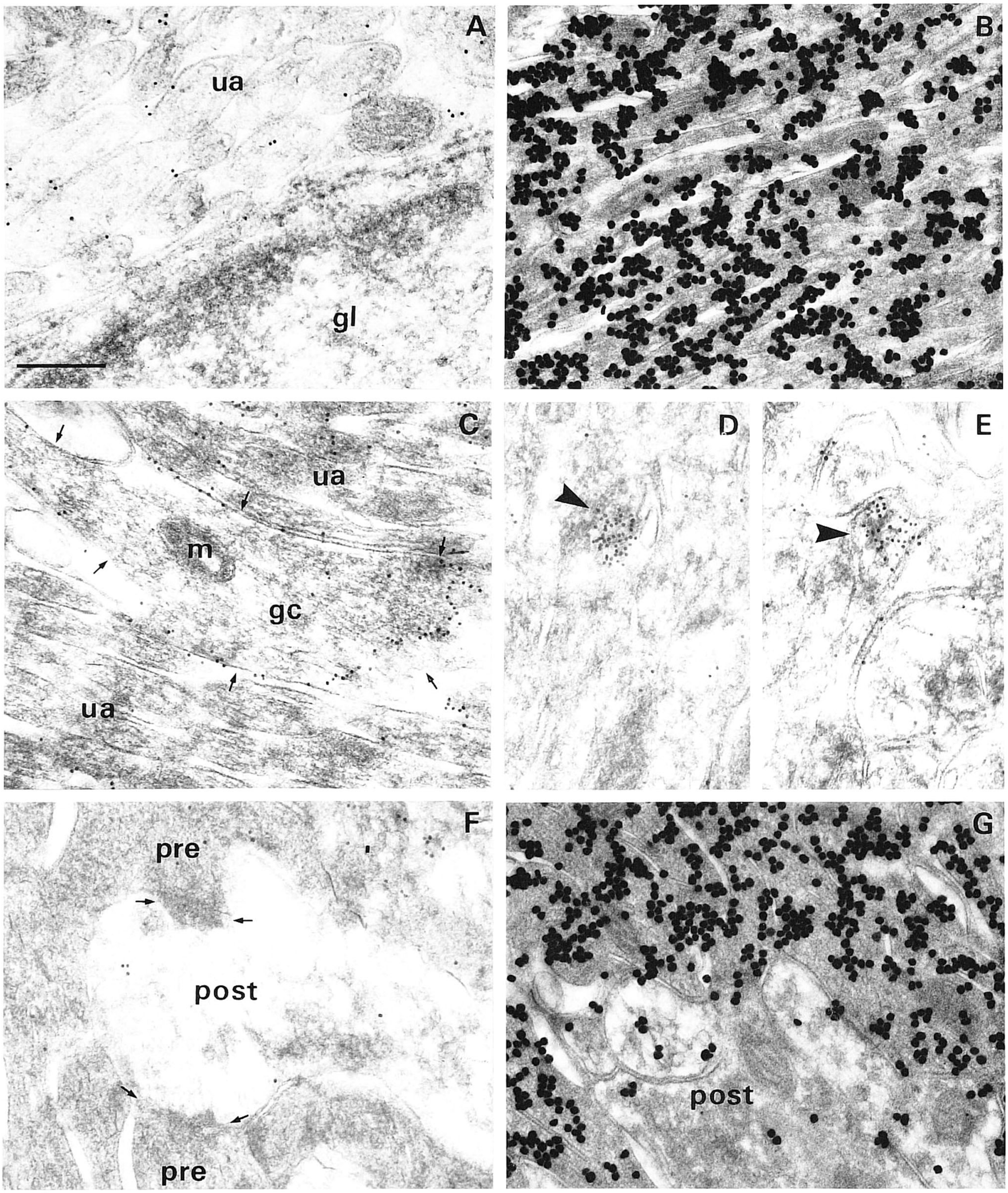

Fig. 6. Immunogold-staining for B-50 (A, C-F) and OMP (B, G) in the nerve fibre layer and glomeruli in six-week-old mouse olfactory bulb. (A) In the fibre layer, B-50 shows a moderate staining density in cross-sectioned primary olfactory axons (ua = unmyelinated axons), whereas OMP (B) shows a uniform high-density labelling of olfactory axons. Glials cells (gl) in the fibre layer show only background staining for B-50. (C-E) Occasionally, a very high density of B-50-labelling is seen within the fibre layer, in irregular, dilated growth-cone-like structures (gc in C indicated by small arrows; m: mitochondrion), or in presumed cross-sectioned filopodia (D, E: arrowheads). In the glomeruli, B-50 staining (F) of primary olfactory terminals is less dense than in the nerve fibre layer, whereas OMP (G) shows a labelling density similar to that in the fibre layer. The arrows in (F) indicate postsynaptic densities (pre: presynaptic; post: postsynaptic element). The high background labelling for OMP may be due to the use of antiserum rather than affinity-purified antibodies. Scale bar = 200 nm.

Table 1. Quantitation of B-50 labelling in mouse olfactory bulb.

Structure:	*UA*	*UA*	*Growth cones*	*Pre*	*Post*	*Dendritic profiles*	*Perikarya*	*Nuclei*	*Mito*	*MA*	*Myelin membrane*
Area:	*NFL*	*GCL*	*All*	*Glom*	*Glom*	*EPL*	*GCL*	*All*	*All*	*GCL/IPL*	*GCL/ILP*
Total surface labelling particles μm^{-2}	63.2 ± 7.7[a]	166 ± 39[b,c]	765 ± 559[b]	19.2 ± 6.4	17.5 ± 6.3	20.2 ± 2.8	12.9 ± 2.8	8.8 ± 1.1	13.6 ± 5.5	19.2 ± 6.1	14.6 ± 5.0
Cytoplasmic labelling particles μm^{-2}	36.5 ± 5.4[d]	51 ± 12[e]	617 ± 485[f]	18.6 ± 4.0	7.9 ± 2.9	15.2 ± 2.8	8.0 ± 2.2	8.7 ± 1.1	5.2 ± 4.0	15.9 ± 5.9	9.1 ± 4.5
Number	41	20	6	40	19	27	8	7	26	10	16
Total area (μm^2)	5.06	.85	1.28	7.75	5.62	6.34	2.78	9.74	1.50	1.40	1.59
Membrane labelling particles μm^{-2}	1.17 ± .24[g]	2.1 ± .26[h]	3.28 ± 1.0	0.60 ± .37	0.77 ± .36	0.34 ± .11	0.52 ± .27	0.16 ± .06	0.28 ± .13	0.15 ± .08	0.18 ± .07
Number	35	19	16	30	29	10	29	3	22	7	26
Total length μm)	52.1	28.6	17.6	13.7	22.2	22.0	27.8	7.0	21.7	14.5	24.9

[a] Significantly different from all other structures at $p < 0.01$.
[b] Significantly different from all other structures at $p < 0.001$, except for the difference between unmyelinated axons in the GCL and growth cones
[c] Significantly different from all other structures at $p < 0.05$.
[d] Significantly different from all other structures at $p < 0.05$ except UA in the GCL and MA ($p < 0.1$).'
[e] Significantly different from all other structures at $p < 0.05$ except UA in the NFL, nuclei, perikarya ($p < 0.1$) and MA ($p < 0.1$).
[f] Significantly different from all other structures.
[g] Significantly different from all other structures at $p < 0.05$, except postsynaptic structures in the GLOM, perikaryal membranes ($p < 0.1$, and nuclear membranes ($p < 0.1$).
[h] Significantly different from all other structures at $p < 0.05$.
UA = unmyelinated axons; MA = myelinated axons; PRE = presynaptic terminals; POST = postsynaptic elements; NFL = fibre layer; GCL = granule cell layer; GLOM = glomeruli; EPL = external plexiform layer; IPL = internal plexiform layer.

protein matrix in these axons (Fig. 6F; Pinching & Powell, 1971; White, 1972). Although this higher density obscured the visibility of synaptic vesicles, it did not affect the detection of the 10 nm gold particles. Overall B-50 immunoreactivity was low in the glomeruli, with the dendritic structures showing a somewhat lower labelling density than the presynaptic primary olfactory terminals (Fig. 6F). Dendritic labelling did not appear to be specifically associated with the plasma membrane or synaptic vesicles. Labelling for OMP in the fibre layer and glomeruli was found in the cytoplasm of olfactory axons and terminals, and appeared to have a similar density in both (Fig. 6B, G). Dendritic structures in the glomeruli also showed some staining above background, which we consider to be due to non-specific staining by the non-affinity purified OMP-antiserum. Periglomerular cells did not show any labelling above background, anywhere within the soma or nucleus (not shown).

The external plexiform layer contained mainly dendritic structures of various diameters, synapses, and a few myelinated axons. Average B-50 immunolabelling was very low, but still appeared somewhat above background (Fig. 7A,B). Dendrites showed very low labelling, both at the membrane or in the cytoplasm. In synaptic structures in the external plexiform layer, the great majority of which are reciprocal dendro-dendritic synapses (Rall *et al.*, 1966), also little labelling was seen (Fig. 7A). The perikarya of mitral and tufted cells showed no immunogold labelling, neither along the plasma membrane nor in organelles (Fig. 7C).

The highest overall B-50 labelling density was observed in the internal plexiform layer (not shown) and granule cell layer (Figs 7D–E, 8), and was restricted to thin non-myelinated axons. These non-myelinated axons are derived from neurons projecting from the piriform cortex and anterior olfactory nucleus onto granule cell dendritic spines (Davis and Macrides, 1981). Surprisingly, in myelinated axons (which were always thicker than the non-myelinated axons), labelling was at background level, as was also observed in other layers of the MOB (Figs 7E, 8). Granule cell somata and dendrites showed background labelling (Figs 7D,F, 8). As granule cells are often closely apposed within small clusters, without any other structures in between, the plasma membranes of two apposed granule cells provided an excellent opportunity to examine B-50 labelling densities on the plasma membranes of neuronal somata. Indeed, labelling density on the somal plasma membranes was very low (Fig. 7F). In synapses, labelling was exclusively found at the presynaptic side, while the postsynaptic element displayed background staining (Figs 7D, 8).

Throughout the MOB, no labelling was seen in oligodendrocytes (including the myelin sheath; not shown), glial cells (Fig. 6A), or endothelial cells (not shown).

Quantification of B-50 immunogold labelling in the MOB

Quantification of B-50 labelling in a variety of profiles throughout the MOB closely reflected the qualitative impression of B-50 labelling in the MOB (Table 1). Total surface labelling per structure (including membrane labelling) in nuclei was similar to the background labelling seen in control-stained sections (see

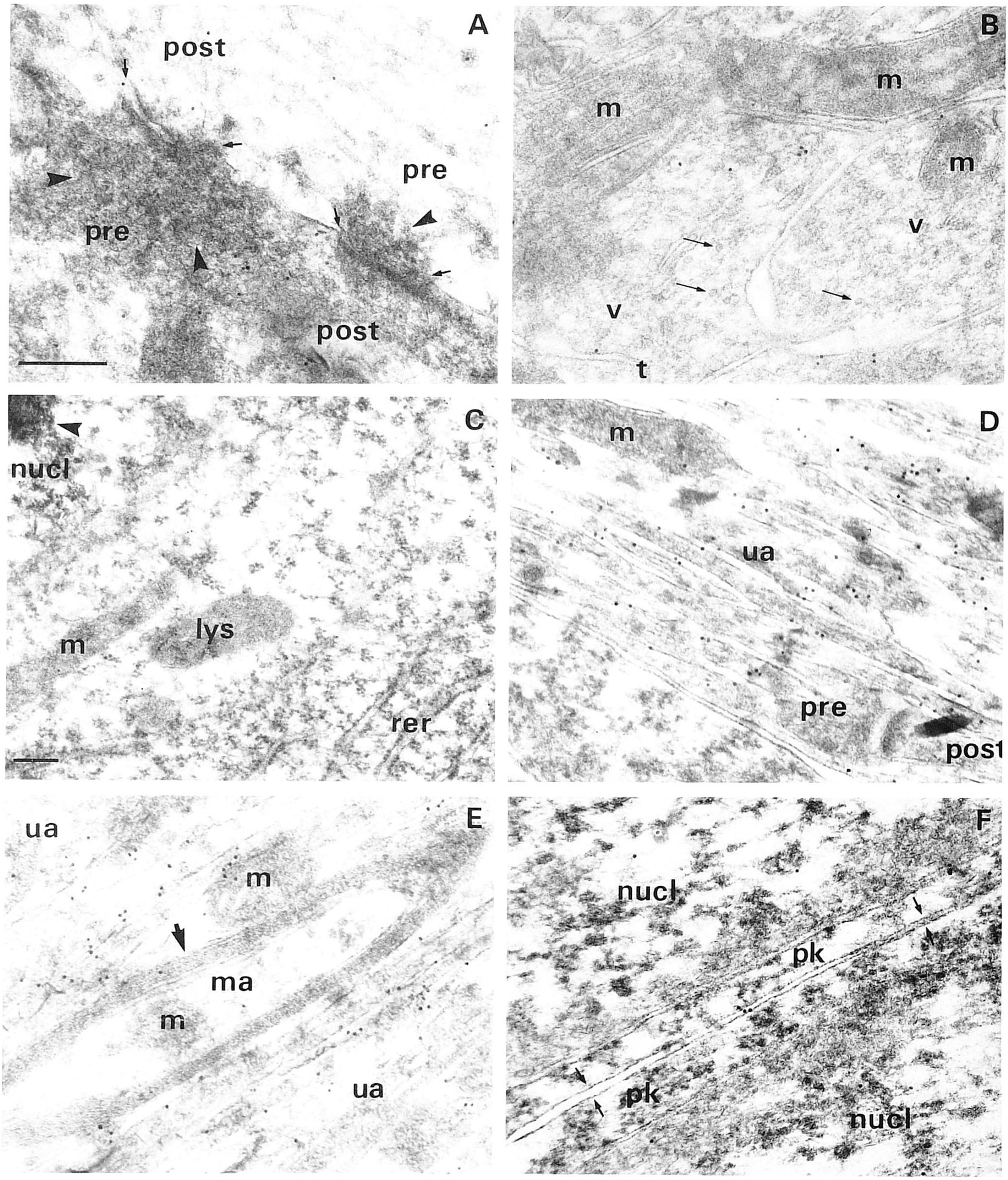

Fig. 7. Immunogold-staining for B-50 in the external plexiform layer (A, B), mitral cells (C) and the GCL (D, E, F) in six-week-old mouse olfactory bulb. A reciprocal dendrodendritic synapse in the external plexiform layer (A) shows a low staining density for B-50 Two adjacent clusters of synaptic vesicles (arrowheads) are seen in both dendritic structures, close to the synaptic clefts (small arrows; pre and post: pre- and postsynaptic side, respectively). (B) Overall staining density for B-50 in the mainly dendritic external plexiform layer is very low (v: vesicle-containing dendritic profiles; the arrows indicate some of the vesicles; m: mitochondria). (C) Mitral cell soma exhibiting background staining (arrowhead: nucleolus; nucl: nucleus; m: mitochondrion; lys: lysosomal structure; rer: rough endoplasmic reticulum; the cytoplasm shows abundant ribosomes). (D, E) In the GCL, a high staining density is associated with thin unmyelinated axons (ua; D: pre: presynaptic element). Postsynaptic dendrites (D: post) and all myelinated axons (ma) show background staining. (F) The apposed plasma membranes (arrows), perikaryal cytoplasm (pk) and nuclei (nucl) of granule cell bodies show background staining only. Scale bars: (A) (for all panels except (C)): = 200 nm. (C) 200 nm.

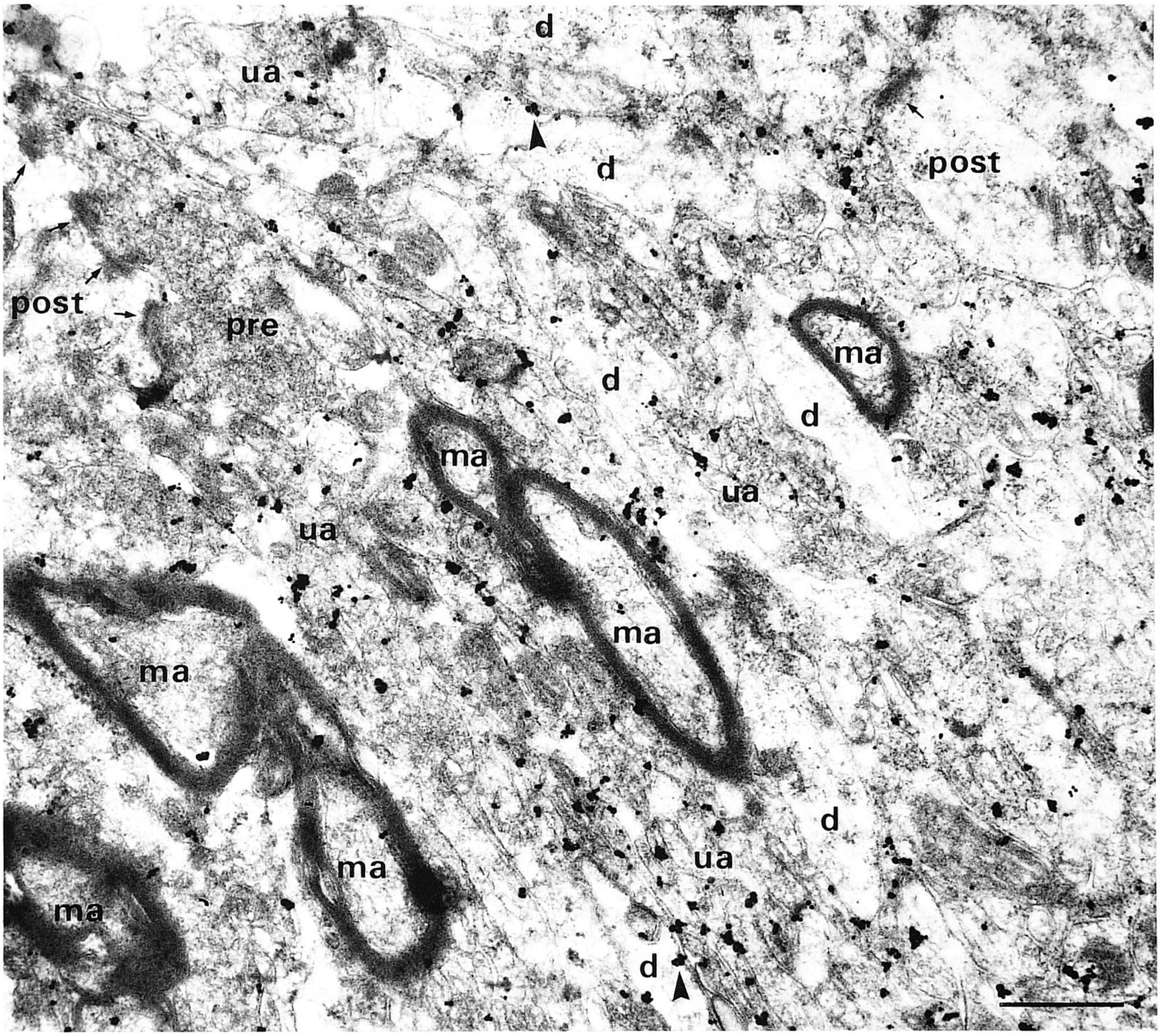

Fig. 8. Overview of B-50 labelling in the GCL neuropil with 1 nm immunogold particles, silver enhanced to 10 nm. The highest labelling density is seen in thin unmyelinated axons (ua). A large presynaptic terminal (pre) mainly contains labelling along its plasma membrane, but not associated with synaptic vesicles. Background labelling (which is higher with this method than with 10 nm gold particles) is seen in myelinated axons (ma), dendritic profiles (d; light matrix) and postsynaptic elements (post). Although labelling efficiency is much higher with 1 nm gold particles (cf. Fig. 6D, E), they usually are aggregated, resulting in a lower spatial resolution of the labelling. Thus, the clusters of particles near the plasma membrane in some of the dendritic structures in this photograph (arrowheads), most likely are due to B-50 abundantly present in the surrounding thin unmyelinated axons. Scale bar = 500 nm.

above). A very high labelling density was found in growth cone-like structures, followed by labelling in thin unmyelinated axons in the granule cell layer neuropil and in the fibre layer. In all other structures, like presynaptic terminals of primary olfactory neurons and postsynaptic endings inside the glomeruli, dendrites, perikarya, mitochondria, myelinated axons, and myelin, labelling density was not significantly elevated above that in the nuclei (Table 1). When only the density of cytoplasmic labelling was determined, the same overall profile of labelling densities was observed (Table 1).

The density of membrane labelling was highest in growth cone-like structures, and second highest in thin unmyelinated axons of the granule cell layer. The unmyelinated axons of the nerve fibre layer showed a level of membrane labelling intermediate between unmyelinated axons of the granule cell layer and most

other structures which did not show labelling above the density observed in perikaryal membranes.

Quantification of the density of total surface labelling for OMP in primary olfactory axons and in their terminals did not reveal any difference (axons: mean density ± SEM: 820 ± 70 particles μm^{-2}; terminals: 760 ± 58 particles μm^{-2}; not significant at the 5% level in a Mann-Whitney U-test).

Discussion

This study demonstrates that B-50 is primarily expressed in some primary olfactory axons and presumptive growth cones in the nerve fibre layer of the olfactory bulb, in unmyelinated axons and presynaptic terminals in the neuropil of the granule cell layer and among periglomerular cells. In the glomeruli and the external plexiform layer low levels of B-50 immunostaining were observed. Within the piriform cortex B-50 staining was low in the LOT, which contains the myelinated mitral and tufted cell axons (Scott *et al.*, 1980), and most intense in the regions of layer I bordering the LOT and layer II. The cytoplasm as well as the membranes of neuronal perikarya, dendrites, and glial cells are virtually devoid of B-50 immunoreactivity.

The distribution of four neural proteins, i.e. OMP, MAP2, NFH and MBP, each exhibiting a well-established cellular localization, was compared with the pattern of B-50 immunostaining in order to facilitate the analysis of the distribution of B-50 in the olfactory bulb. The present findings confirm the uniform cytoplasmic location of OMP (Menco, 1989) in the primary olfactory axons in the nerve fibre layer and their terminals in the glomeruli. Comparison of the distribution of OMP and B-50 shows a clear decline in B-50 immunostaining intensity going from the olfactory axons in the nerve fibre layer to the primary olfactory terminals in the glomeruli. This is consistent with the notion that establishment of synaptic contacts between primary olfactory neurons on their target dendrites in the glomeruli during postnatal development and following olfactory nerve lesion (Verhaagen *et al.*, 1990b) results in a down regulation of B-50 expression in primary olfactory neurons. Thus, the patchy B-50 staining in the nerve layer indicates that this structure is composed of two populations of axons: relatively immature (B-50 positive) axons that have not yet formed synapses in the olfactory bulb and B-50 negative axons projecting into glomeruli, where they have established synapses. In view of this we are confident that the relatively high number of irregular membrane-rich B-50 positive structures in the nerve fibre layer represent growth cones. some of the larger growth cones are clearly continuous with olfactory axons and are reminiscent of B-50 stained growth cones in neonatal hippocampus (Van Lookeren Campagne *et al.*, 1990) and in tissue culture (Ramakers *et al.*, 1991b). The smaller B-50 immunoreactive structures in the nerve fibre layer probably represent growth cone filopodia, parts of growth cones most enriched in B-50 (Meiri *et al.*, 1988; Ramakers *et al.*, 1991b).

The dendritic marker MAP2 (Bernhardt & Matus, 1984; in the olfactory bulb: Viereck *et al.*, 1989) and B-50 are differentially expressed indicating that B-50 expression is low if not absent from dendrites. EM analysis indeed demonstrates the virtual absence of B-50 from dendrites in glomeruli, the granule cell layer neuropil and the external plexiform layer. This confirms previous observations in adult hippocampus and central grey (Gispen *et al.*, 1985; Van Lookeren Campagne *et al.*, 1990, 1991a) and supports the view that B-50 is preferentially directed to axonal processes (Goslin *et al.*, 1988). Although studies in the adult neostriatum indicate that B-50 could be involved in dendritic remodelling (DiFiglia *et al.*, 1990), we did not find evidence for this in our study. With regard to the proposed involvement of B-50 in the regulation of transmitter release (Dekker *et al.*, 1989b), it is of interest to note that B-50 is absent from the numerous reciprocal dendro-dendritic synapses (Rall *et al.*, 1966; Jackowski *et al.*, 1978) in the glomeruli and the external plexiform layer. This indicates that B-50 does not participate in transmitter release in this particular type of synapse.

The NFH and MBP antibodies appeared to be excellent tools to identify the projections of the myelinated mitral- and tufted cell fibres to the piriform cortex. The monoclonal neurofilament antibody recognizes epitopes in NFH exclusively expressed in myelinated fibres as shown by double immunostaining with MBP antibodies. Our findings indicate that B-50 is absent from the myelinated mitral and tufted cell fibre tracts in the granule cell layer and in the piriform cortex. This was confirmed by the ultrastructural analysis in the MOB. The high level of B-50 labelling in the granule cell layer is due to B-50 expression in thin unmyelinated afferent axons, which appear to terminate largely on granule cell dendritic spines. The distribution of these thin unmyelinated fibres most closely matches that of the preterminal axonal arbors of centrifugal projections by pyramidal neurons of the piriform cortex (Davis & Macrides, 1981). Interestingly, a large proportion of these latter neurons continues to express high levels of B-50 mRNA in adulthood (De la Monte *et al.*, 1989; Bendotti *et al.*, 1991). As B-50 immunostaining in the pyramidal cell somata was negligible, it seems likely that B-50 in these neurons is concentrated in the target area in the MOB. Synaptic contacts between these B-50 expressing axons and B-50 negative dendritic spines of granule cells were observed frequently.

In the piriform cortex B-50 is most abundant in the

superficial part of layer Ia, a location where the preterminal unmyelinated axon branches of the mitral and tufted cells arise from the LOT and synapse on dendrites of piriform cortex neurons (Scott *et al.*, 1980). The persistent expression of B-50 mRNA in adult mitral cells has been proposed to reflect synaptic remodelling in the mitral cell dendrites in the glomeruli and/or in their axonal projections in the piriform cortex (Verhaagen *et al.*, 1990a). Our present observations of an absence of B-50 from mitral cell dendrites and its light microscopic abundance in the central projection area support transport of B-50 from the mitral cell somata to their nerve endings in the piriform cortex.

High levels of B-50 expression in thin unmyelinated axons are apparently not unique to the mouse olfactory system, since a similar distribution has been described for the hippocampus (Van Lookeren Campagne *et al.*, 1990), the periaquaductal grey (Van Lookeren Campagne *et al.*, 1991a) and the neostriatum (DiFiglia *et al.*, 1990). In all these brain areas the thin unmyelinated axons were located upstream from the presynaptic terminal and correspond to the terminal arbors which arise from myelinated axons when they reach their target neuropil. The prevalence of B-50 in thin unmyelinated axons in the granule cell layer and presumably also in the piriform cortex may be related to remodelling of these processes as part of the high levels of ongoing synaptic plasticity reported in the olfactory system (Leon, 1987; Haberly & Bower, 1989). In accordance with the implication of B-50 in synaptic plasticity and neurite outgrowth, we propose that the thin, unmyelinated preterminal axonal branches potentially represent sites of high neuronal plasticity.

Acknowledgements

The authors wish to thank Dr A. Matus (Friedrich Miescher Institut, Basel, Switzerland) for the AP14 monoclonal antibody, Dr F.C.S. Ramaekers (Dept. Mol. Cell Biology, University of Limburg, Maastricht, The Netherlands) for the RNF 402 monoclonal antibody, and Dr M. van Berlo (Dept. Virology, Veterinary Faculty, University of Utrecht) for the antibody against myelin basic protein.

References

ALEXANDER, K. A., CIMLER, B. M., MEIER, K. E. & STORM, D. R. (1987) Regulation of calmodulin binding to P-57. *Journal of Biological Chemistry* **62**, 6108–13.

BENDOTTI, C., SERVADIO, A. & SAMANIN, R. (1991) Distribution of GAP-43 mRNA in the brain stem of adult rats as evidenced by in situ hybridization: localization within monoaminergic neurons. *Journal of Neuroscience* **11**, 600–7.

BENOWITZ, L. I. & ROUTTENBERG, A. (1987) A membrane phosphoprotein associated with neural development, axonal regeneration, phospholipid metabolism and synaptic plasticity. *Trends in Neuroscience* **12**, 527–32.

BENOWITZ, L. I., APOSTOLIDES, P. J., PERRONE BIZZOZERO, J., FINKLESTEIN, S. P. & ZWIERS, H. (1988) Anatomical distribution of the growth-associated protein GAP-43/B-50 in the adult rat brain. *Journal of Neuroscience* **8**, 339–52.

BERNHARDT, R. & MATUS, A. (1984) Light and electron microscopic studies of the distribution of microtubule-associated protein 2 in rat brain: a difference between the dendritic and axonal cytoskeletons. *Journal of Comparative Neurology* **226**, 203–21.

DANSCHER, G. (1981) Localization of gold in biological tissue. A photochemical method for light and electron microscopy. *Histochemistry* **71**, 81–8.

DAVIS, B. J. & MACRIDES, F. (1981) The organization of centrifugal projections from the anterior olfactory nucleus, ventral hippocampal rudiment, and piriform cortex to the main olfactory bulb in the hamster: an autoradiographic study. *Journal of Comparative Neurology* **203**, 475–93.

DE GRAAN, P. N. E., VAN HOOFF, C. O. M., TILLY, B. C., OESTREICHER, A. B., SCHOTMAN, P. & GISPEN, W. H. (1985) Phosphoprotein B-50 in nerve growth cones from fetal rat brain. *Neuroscience Letters* **61**, 235–41.

DEKKER, L. V., DE GRAAN, P. N. E., DE WIT, M., HENS, J. J. H. & GISPEN, W. H. (1989a) Depolarization-induced phosphorylation of the protein kinase C substrate B-50 (GAP-43) in rat cortical synaptosomes. *Journal of Neurochemistry* **54**, 1645–52.

DEKKER, L. V., DE GRAAN, P. N. E., OESTREICHER, A. B., VERSTEEG, D. H. G. & GISPEN, W. H. (1989b) Inhibition of noradrenaline release by antibodies to B-50 (GAP-43). *Nature* **342**, 74–6.

DE LA MONTE, S. M., FEDEROFF, H. J., NG, S.-C., GRABCYK, E. & FISHMAN, M. C. (1989) GAP-43 gene-expression during development: persistence in a distinctive set of neurons in the mature central nervous system. *Developmental Brain Research* **46**, 161–8.

DIFIGLIA, M., ROBERTS, R. C. & BENOWITZ, L. I. (1990) Immunoreactive GAP-43 in the neuropil of adult rat neostriatum: localization in unmyelinated fibres, axon terminals, and dendritic spines. *Journal of Comparative Neurology* **302**, 992–1001.

FARBMAN, A. I. & MARGOLIS, F. L. (1980) Olfactory marker protein ontogeny: immunohistochemical localization. *Developmental Biology* **74**, 205–15.

GISPEN, W. H., LEUNISSEN, J. L. M., OESTREICHER, A. B., VERKLEIJ, A. J. & ZWIERS, H. (1985) Presynaptic localization of B-50 phosphoprotein: the ACTH sensitive protein kinase substrate involved in rat brain polyphosphoinositide metabolism. *Brain Research* **328**, 381–5.

GOSLIN, K., SCHREYER, D. J., SKENE, J. H. P. & BANKER, G.

(1988) Development of neuronal polarity: GAP-43 distinguishes axonal from dendritic growth cones. *Nature* **336**, 672–4.

GRAZIADEI, P. P. C. & MONTI-GRAZIADEI, G. A. (1978) The olfactory system: a model for the study of neurogenesis and axon regeneration in mammals. In *Neuronal Plasticity* (edited by COTMAN, C. W.) pp. 288–321. New York: Raven Press.

HABERLY, L. B. & BOWER, J. M. (1989) Olfactory cortex: model circuit for study of associative memory? *Trends in Neuroscience* **12**, 258–64.

HUMBEL, B. & MÜLLER, M. (1986) Freeze substitution low-temperature embedding. In *Science of Biological Specimen Preparation 1985* (edited by MÜLLER, M., BECKER, R. P., BOYDE, A. & WOLOSEWICK, J. J.) pp. 175–83. AMF O'Hare, Il: SEM, Inc.

JACKOWSKI, A., PARNAVELAS, J. G. & LIEBERMAN, A. R. (1978) The reciprocal synapse in the external plexiform layer of the mammalian olfactory bulb. *Brain Research* **159**, 17–28.

KATZ, F., ELLIS, L. & PFENNINGER, K. H. (1985) Nerve growth cones isolated from fetal rat brain. III. Calcium-dependent protein phosphorylation. *Journal of Neuroscience* **5**, 1402–11.

LEON, M. (1987) Plasticity of olfactory output circuits related to early olfactory learning. *Trends in Neuroscience* **10**, 434–8.

LOVINGER, D. M., AKERS, R. F., NELSON, R. B., BARNES, C. A., MCNAUGHTON, B. L. & ROUTTENBERG, A. (1985) A selective increase in phosporylation of protein F1, a protein kinase C substrate, directly related to three day growth of long term synaptic enhancement. *Brain Research* **343**, 137–43.

MARGOLIS, F. L. (1972) A brain protein unique to the olfactory bulb. *Proceedings of the National Academy of Sciences (USA)* **69**, 1221–4.

MEIRI, K. F., PFENNINGER, K. H. & WILLARD, M. (1986) Growth-associated protein GAP-43, a polypeptide that is induced when neurons extend axons, is a component of growth cones and corresponds to pp46, a major polypeptide of a subcellular fraction enriched in growth cones. *Proceedings of the National Academy of Sciences (USA)* **83**, 3537–41.

MEIRI, K. F., WILLARD, M. & JOHNSON, M. I. (1988) Distribution and phosphorylation of growth-associated protein GAP-43 in regenerating sympathetic neurons in culture. *Journal of Neuroscience* **8**, 2571–81.

MEIRI, K. F., BICKERSTAFF, L. E. & SCHWOB, J. (1991) Monoclonal antibodies show that kinase C phosphorylation of GAP-43 during axogenesis is both spatially and temporally restricted in vivo. *Journal of Cell Biology* **112**, 991–1005.

MENCO, B. P. (1989) electron-microscopic demonstration of olfactory marker protein with protein G-gold in freeze-substituted, Lowicryl K11M-embedded rat olfactory receptor cells. *Cell and Tissue Research* **256**, 275–81.

MIRAGALL, F., KADMON, G., HUSMANN, M. & SCHACHNER, M. (1988) Expression of cell adhesion molecules in the olfactory system of the adult mouse: presence of the embryonic form of N-CAM *Developmental Biology* **129**, 516–31.

MONTI-GRAZIADEI, G. A., MARGOLIS, F. L., HARDING, J. W. & GRAZIADEI, P. P. C. (1977) Immunocytochemistry of olfactory marker protein. *Journal of Histochemistry and Cytochemistry* **15**, 1311–16.

NEVE, R. L., FINCH, E. A., BIRD, E. D. & BENOWITZ, L. I. (1988) Growth-associated protein GAP-43 is expressed selectively in associative regions of the adult human brain. *Proceedings of the National Academy of Sciences (USA)* **85**, 3638–42.

OESTREICHER, A. B., VAN DONGEN, C. J., ZWIERS, H. & GISPEN, W. H. (1983) Affinity-purified anti-B-50 protein antibody: interference with the function of the phosphoprotein B-50 in synaptic plasma membranes. *Journal of Neurochemistry* **41**, 331–40.

OTTERSEN, O. P. (1989) Quantitative electron microscopic immunocytochemistry of neuroactive amino acids. *Anatomy and Embryology* **180**, 1–15.

PINCHING, A. J. & POWELL, T. P. S. (1971) The neuropil of the glomeruli of the olfactory bulb. *Journal of Cell Science* **9**, 347–77.

RALL, W., SHEPHERD, G. M., REESE, T. S. & BRIGHTMAN, M. W. (1966) Dendrodendritic synaptic pathway for inhibition in the olfactory bulb. *Experimental Neurology* **14**, 44–56.

RAMAKERS, G. J. A., RAADSHEER, F. C., CORNER, M. A., RAMAEKERS, F. C. S. & VAN LEEUWEN, F. W. (1991a) Development of neurons and glial cells in cerebral cortex, cultured in the presence or absence of bioelectric activity. I. Morphological observations. *European Journal of Neuroscience* **3**, 154–61.

RAMAKERS, G. J. A., OESTREICHER, A. B., WOLTERS, P. S., VAN LEEUWEN, F. W., DE GRAAN, P. N. E. & GISPEN, W. H. (1991b) Developmental changes in B-50 (GAP-43) in primary cultures of cerebral cortex: B-50 immunolocalization, axonal elongation rate and growth cone morphology. *International Journal of Developmental Neuroscience* **9**, 215–30.

RAMAKERS, G. J. A., DE GRAAN, P. N. E., OESTREICHER, A. B., BOER, G. J., CORNER, M. A. & GISPEN, W. H. (1991c) Developmental changes in B-50/GAP-43 in primary cultures of cerebral cortex: content and phosphorylation of B-50. *International Journal of Developmental Neuroscience* **9**, 231–41.

ROSENTHAL, A., CHAN, S. Y., HENZEL, W., HASKELL, C., KUANG, W. J., CHEN, E., WILCOX, J. N., ULLRICH, A., GOEDDEL, D. V. & ROUTTENBERG, A. (1987) Primary structure and mRNA localization of protein F1, a growth-related protein kinase C substrate associated with synaptic plasticity. *EMBO Journal* **6**, 3641–6.

SCHWOB, J. E., FARBER, N. B. & GOTTLIEB, D. I. (1986) Neurons of the olfactory epithelium in adult rats contain vimentin. *Journal of Neuroscience* **6**, 208–17.

SCOTT, J. W., MCBRIDE, R. L. & SCHNEIDER, S. P. (1980) The organization of projections from the olfactory bulb to the piriform cortex and olfactory tubercle in the rat. *Journal of Comparative Neurology* **194**, 519–534.

SIEGEL, S. & CASTELLAN, N. J. (1988) Nonparametric statistics for the behavioural sciences. New York: McGraw-Hill.

SKENE, J. H. P. (1989) Axonal growth-associated proteins. *Annual Review of Neuroscience* **12**, 127–56.

SKENE, J. H. P. & WILLARD, M. (1981a) Changes in axonally transported proteins during axon regeneration in toad retinal ganglion cells. *Journal of Cell Biology* **89**, 86–95.

SKENE, J. H. P. & WILLARD, M. (1981b) Axonally transported proteins associated with axon growth in rabbit central and peripheral nervous system. *Journal of Cell Biology* **89**, 96–103.

SKENE, J. H. P., JACOBSON, R. D., SNIPES, G. J., MCGUIRE, C. B., NORDEN, J. J. & FREEMAN, J. A. (1986) A protein induced during nerve growth (GAP-43) is a major component of growth-cone membranes. *Science* **233**, 783–6.

STRITTMATTER, S. M., VALENZUELA, D., KENNEDY, T. E., NEER, E. J. & FISHMAN, M. C. (1990) G_o is a major growth cone protein subject to regulation by GAP-43. *Nature* **344**, 836–41.

VAN DER SLUIS, P. J., POOL, C. W. & SLUITER, A. A. (1987) Press-blotting on gelatin-coated nitrocellulose membranes. A method for sensitive quantitative immunodetection of peptides after gel isoelectric focusing. *Journal of Immunological Methods* **104**, 65–71.

VAN BERGEN EN HENEGOUWEN, P. M. P. (1989) Immunogold labelling of ultrathin cryosections. In *Colloidal Gold: Principles, Methods, and Applications* **1**, 191–216.

VAN HOOFF, C. O. M., DE GAAN, P. N. E., BOONSTRATA, J., OESTREICHER, A. B., SCHMIDT-MICHELS, M. H. & GISPEN, W. H. (1986) Nerve growth factor enhances the level of the protein kinase C substrate B-50 in pheochromacytoma PC12 cells. *Biochemical and Biophysical Research Communications* **139**, 644–51.

VAN HOOFF, C. O. M., DE GRAAN, P. N. E., OESTREICHER, A. B. & GISPEN, W. H. (1988) B-50 phosphorylation and polyphosphoinositide metabolism in nerve growth cone membranes. *Journal of Neuroscience* **8**, 1789–95.

VAN LOOKEREN CAMPAGNE, M., OESTREICHER, A. B., VAN BERGEN EN HENEGOUWEN, P. M. P. & GISPEN, W. H. (1990) Ultrastructual double localization of B-50/GAP-43 and synaptophysin (p38) in the neonatal and adult rat hippocampus. *Journal of Neurocytology* **19**, 948–61.

VAN LOOKEREN CAMPAGNE, M., OESTREICHER, A. B., BUMA, P., VERKLEIJ, A. J. & GISPEN, W. H. (1991a) Ultrastructural localization of adrenocorticotrophic hormone and the phosphoprotein B-50/growth-associated protein 43 in freeze-substituted, lowicryl HM20-embedded mesencephalic central grey substance of the rat. *Neuroscience* **42**, 517–29.

VAN LOOKEREN CAMPAGNE, M., OESTREICHER, A. B., DE GRAAN, P. N. E. & GISPEN, W. H. (1991b) On the role of B-50 in nerve growth cone function. In *The Nerve Growth Cone* (edited by KATER, S. B., LETOURNEAU, P. C. & MACAGNO, E. R. pp. 97–109. New York: Raven Press.

VERHAAGEN, J., OESTREICHER, A. B., GISPEN, W. H. & MARGOLIS, F. L. (1989) The expression of the growth associated protein B50/GAP43 in the olfactory system of neonatal and adult rats. *Journal of Neuroscience* **9**, 683–91.

VERHAAGEN, J., GREER, C. A. & MARGOLIS, F. L. (1990a) B50/GAP43 gene expression in the rat olfactory system during postnatal development and aging. *European Journal of Neuroscience* **2**, 397–407.

VERHAAGEN, J., OESTREICHER, A. B., GRILLO, M., KHEW-GOODALL, Y. S., GISPEN, W. H. & MARGOLIS, F. L. (1990b) Neuroplasticity in the olfactory system: differential effects of bulbectomy and peripheral lesion of the primary olfactory pathway on the expression of the growth-associated protein B-50/GAP43 and olfactory marker protein. *Journal of Neuroscience Research* **26**, 31–44.

VIERECK, C., TUCKER, R. P. & MATUS, A. (1989) The adult rat olfactory system expresses microtubule-associated proteins found in the developing brain. *Journal of Neuroscience* **9**, 3547–57.

WHITE, E. L. (1972) Synaptic organization in the olfactory glomerulus of the mouse. *Brain Research* **37**, 69–80.